

## Ionization of Rydberg atoms in thermal collisions with polar molecules

Toshizo Shirai

*Tokai Research Establishment, Japan Atomic Energy Research Institute, Tokai-mura 319-11, Japan*

Hiroki Nakamura

*Division of Theoretical Studies, Institute for Molecular Science, Myodaiji, Okazaki 444, Japan*

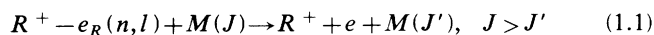
(Received 4 June 1987)

The title process with simultaneous rotational deexcitation of molecules was investigated theoretically by using the semiquantal approximation. The dipole Born and dipole Glauber differential cross sections were employed for the electron-molecule rotational deexcitation process. Numerical applications were made to the following systems: Xe + CO, HCl, HF, and LiF. A comparative study of the two approximations was carried out concerning the dependences of the cross sections on the following various quantities:  $n$  (principal quantum number),  $J$  (initial rotational quantum number),  $\Delta J$  (rotational quantum number change),  $D$  (dipole moment),  $V$  (relative collision velocity). As the molecular dipole moment becomes larger, there appears a prominent difference in the  $n$  dependence of the cross section. The Glauber approximation brings about a decrease in the cross section and yields a sawlike  $n$  dependence in contrast to a steplike  $n$  dependence in the case of the Born approximation. In the collisions involving lowly excited Rydberg atoms, ionization with simultaneous dipole-forbidden transition of a molecule becomes dominant compared to the ionization with simultaneous dipole-allowed transition. The cross section was found to be inversely proportional to the relative collision velocity; thus the ionization rate becomes independent of temperature. A comparison was also made between the experiment for the ionization rate at 300 K for Xe(27f) + HF and Xe(31f) + HCl.

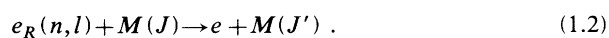
### I. INTRODUCTION

In the past ten years numerous experimental and theoretical studies<sup>1</sup> have been made of collisional depopulation of Rydberg, or highly excited, atoms in thermal collisions with polar molecules. The experimental results<sup>2</sup> show that the collisional depopulation occurs by three distinct processes, namely,  $n$ -changing collisions,  $l$ -changing collisions, and ionization collisions. In order to elucidate the mechanisms of these processes theoretically, not only the approximate quantum-mechanical approaches<sup>3</sup> within the impulse approximation but also the purely classical treatment<sup>4</sup> have been applied.

In this paper ionization collision between a Rydberg atom  $R$  and a rotationally excited polar molecule  $M(J)$  at room temperature (i.e.,  $T=300$  K),



is examined theoretically. Here  $R^+$  denotes the ion core of  $R$  and  $e_R(n, l)$  the Rydberg electron in the state with specified principal ( $n$ ) and azimuthal ( $l$ ) quantum numbers. Ionization occurs mainly owing to the energy transfer from molecular rotation to atomic excitation, because the energy transfer from relative translational motion to atomic excitation is much less effective. Therefore the key mechanism for the ionization is the rotational de-excitation process,



As far as the authors know, the approximate quantum-mechanical calculations carried out so far employed the dipole Born approximation<sup>5</sup> for the process (1.2). In or-

der to take into account the higher-order corrections, however, the dipole Born approximation should be replaced by a more sophisticated one. Especially when the molecule is strongly polar, the validity of the Born approximation becomes questionable. We employed here the Glauber approximation. The dipole Glauber differential cross section<sup>6</sup> (DCS) becomes the same as the dipole Born DCS when the molecular dipole moment is weak, and also reproduces well the results of the close-coupling calculations even when the molecular dipole moment becomes larger. Besides, it should be noted that the dipole-forbidden transitions can also be dealt with by the dipole Glauber approximation. In a recent paper,<sup>7</sup> Pesnelle *et al.* reported the importance of the rotational deexcitation with  $\Delta J \equiv J - J' > 1$  in the ionization collisions of low Rydberg He atoms with  $\text{NH}_3$ . Using the semiquantal approximation,<sup>8</sup> we have carried out the calculations of the ionization collisions between the Rydberg Xe atoms and the polar molecules CO, HF, HCl, and LiF. Both Glauber and Born DCS's for the rotational deexcitation process (1.2) were employed for comparison.

In a previous paper<sup>9</sup> (referred to as I hereafter) we proposed a new semiquantal cross section formula to be applicable to the general case where the DCS for electron-neutral atom (molecule) scattering depends not only on the momentum transfer but also on the relative velocity. A brief summary of the theory is given in Sec. II. In Sec. III the calculated results and discussions are presented for the following systems: Xe(50) + HF( $J$ ), Xe(50,  $l$ ) + HF, and Xe( $n$ ) + CO, HCl, HF, and LiF. Experimental<sup>10,11</sup> and theoretical<sup>4</sup> ionization rates for

Xe(27f) + HF and Xe(31f) + HCl at 300 K are compared with the present results. In the present treatment, the Rydberg atom is assumed to be hydrogenic and the polar molecule is taken to be a rigid rotor.

## II. THEORY

During the collision between a Rydberg atom and a neutral particle (atom or molecule), the neutral particle does not interact simultaneously with both the Rydberg electron and its parent ion core. Owing to the charge neutrality, the interaction between the Rydberg atom and the neutral particle becomes effective only in a small region compared to the dimension of the Rydberg atom. The Rydberg electron and the parent ion are thus assumed to be independent scattering centers. The impulse approximation is appropriate to describe such a characteristic collision. The binary-encounter approximation for the form factor of the Rydberg atom is employed as an additional approximation.<sup>12</sup> This approximation is considered to be quite good, because the momentum transferred to the Rydberg electron is large compared to its own momentum. In the present treatment the parent ion does not play any important role in the collision other than the role of determining the momentum distribution of the Rydberg electron. Thus, the semiquantal approximation used in the present calculations is a kind of combination of the impulse and the binary-encounter approximations.

The semiquantal cross section formula proposed by

Flannery<sup>8</sup> was rewritten in I in the form more useful in practice. A mass-disparity approximation (i.e., neglect of the ratio of mass of electron to that of  $R$  and  $M$ ) is used without introducing any serious error. The following is a summary of the notations used in this paper:  $m$  is the mass of the electron;  $\mu$ , the reduced mass of the  $R$ - $M$  system;  $p_{i,f}$ , the initial and final momentum of the relative motion in the  $R$ - $M$  system;  $p$ , the momentum transfer;

$$p_{\max,\min} = |p_i \pm p_f| \\ = |p_i \pm [p_i^2 - 2(\epsilon_n + \Delta)]^{1/2}| ;$$

$\epsilon_n$ , the ionization potential of  $R(n,l)$ ;  $\Delta$ , the difference of the initial and final rotational energies ( $\Delta > 0$  for excitation and  $\Delta < 0$  for deexcitation);  $\sigma_{JJ'}(p,v)$ , the DCS for the collision (1.2);  $V$ , the initial velocity of the relative motion of the  $R$ - $M$  system;  $\epsilon$ , the internal energy transferred to  $R$ ;

$$\epsilon_{\max} = -p^2/2\mu + Vp - \Delta ; \\ \epsilon_{\min} = \begin{cases} -p^2/2\mu - Vp - \Delta & \text{for } 0 \leq p \leq p_{\min} , \\ \epsilon_n & \text{for } p_{\min} \leq p \leq p_{\max} ; \end{cases}$$

$\mathcal{F}_{nl}(u)$ , the velocity ( $u$ ) distribution function of  $e_R(n,l)$ ; and  $u_n$ , the average orbital velocity of  $e_R(n,l)$ .

The cross-section formula, Eq. (2.37) of I, for the ionization collision (1.1) is expressed within the mass-disparity approximation as follows:

$$\sigma_{nl,J,J'}(V) = \frac{2\pi}{(mV)^2} \int_0^{p_{\max}} p dp \int_{v_m^2}^{\infty} \sigma_{J,J'}(p,v) dv^2 \int_{\epsilon_{\min}}^{\epsilon_{\max}} \frac{d^2F_{nl}(p,v,\epsilon)}{d\epsilon dv^2} d\epsilon , \quad (2.1)$$

where the last integrand is newly introduced and defined by

$$\frac{d^2F_{nl}(p,v,\epsilon)}{d\epsilon dv^2} = \frac{1}{2\pi p} \int_{u_-}^{u_+} \frac{u \mathcal{F}_{nl}(u) du}{[(u_+^2 - u^2)(u^2 - u_-^2)]^{1/2}} . \quad (2.2)$$

The other quantities are the same as in I:  $v_m = p/2m + \Delta/p$ ,  $u_{\pm} = v^2 + C \pm 2[B(v^2 - v_m^2)]^{1/2}$ ,  $C = V^2 - 2v(p, \epsilon)v_m$ ,  $B = V^2 - v(p, \epsilon)^2$ , and  $v(p, \epsilon) = p/2\mu + (\epsilon + \Delta)$ . If the DCS's  $\sigma_{J,J'}(p,v)$  are independent of  $v$ , the order of the integrals with respect to  $v$  and  $\epsilon$  can be changed, and the integral over  $v^2$  can be carried out analytically. Integrating Eq. (2.2) over  $v^2$ , we can obtain the following expression for the density of the binary-encounter form factor:

$$\frac{dF_{nl}(p,\epsilon)}{d\epsilon} = \int_{v_m^2}^{\infty} \frac{d^2F_{nl}(p,v,\epsilon)}{d\epsilon dv^2} dv^2 \\ = \frac{1}{2p} \int_{u(p,\epsilon)}^{\infty} u \mathcal{F}_{nl}(u) du , \quad (2.3)$$

where

$$u(p,\epsilon) = |\epsilon/p - p/2m| .$$

Taking an average of Eq. (2.3) with respect to  $l$  [see Eq. (2.42) of I], we have

$$\frac{dF_n(p,\epsilon)}{d\epsilon} = \frac{1}{n^2} \sum_l (2l+1) \frac{dF_{nl}(p,\epsilon)}{d\epsilon} \\ = \frac{2^4}{3\pi} \frac{1}{2pu_n} [u(p,\epsilon)^2/u_n^2 + 1]^{-3} . \quad (2.4)$$

Thus the quantity defined in Eq. (2.2) can be regarded as a velocity-dependent density of the binary-encounter form factor.

In the dipole Glauber approximation, not only the dipole transition  $\Delta J = J - J' = 1$  but also other nondipole transitions  $\Delta J > 1$  can occur and induce the ionization of the Rydberg atom. Therefore, a summation with respect to  $\Delta J$  and an average over the rotational distribution at a given temperature  $T$  are necessary to be taken to obtain the thermally averaged ionization cross section,

$$\bar{\sigma}_{nl}(V) = \sum_{\Delta J=1}^{\infty} \sum_{J=\max(\Delta J, J^*)}^{\infty} f_J \sigma_{nl,J,J-\Delta J}(V) , \quad (2.5)$$

where

$$f_J = (2J+1)\exp[-BJ(J+1)/kT] / \sum_{J=0}^{\infty} (2J+1)\exp[-BJ(J+1)/kT], \quad (2.6)$$

with  $B$  the rotational constant of the polar molecule and  $k$  the Boltzmann's constant. Here  $J^*$  is the smallest rotational quantum number which satisfies the condition

$$\Delta J(2J^*+1-\Delta J)B \geq \varepsilon_n, \quad (2.7)$$

where the left-hand side represents the deexcitation energy in the transition from  $J^*$  to  $J^* - \Delta J$ .

The ionization rate constant is given as

$$K_{nl}(T) = \int_0^{\infty} V \bar{\sigma}_{nl}(V) f(V) dV, \quad (2.8)$$

where  $f(V)$  is the Boltzmann distribution function given by

$$f(V) = (\mu/2\pi kT)^{3/2} 4\pi V^2 \exp(-\mu V^2/2kT). \quad (2.9)$$

It is useful to later discussion to briefly summarize the findings in I concerning the ionization with simultaneous deexcitation in the low-energy collisions (see Sec. III B of I). By taking into account the fact that the electron-velocity distribution function  $\mathcal{F}_{nl}(u)$  with high  $n$  reaches a maximum at  $u \simeq u_n$  and rapidly decreases when  $u > u_n$ , we estimated an effective integral domain of  $p$ . Since the integral over  $u$  in Eq. (2.2) becomes significant only when  $u_-$  can be zero, the effective domain of  $p$  is determined from a condition that the minimum value of  $u_- (= |\mathbf{v} - \mathbf{V}|)$  is equal to zero. Finally, we obtain the following effective domain of  $p$  [see Eq. (3.11) of I]:

$$p^+ \geq p \geq p^-, \quad (2.10)$$

where

$$p^{\pm} = m[(V^2 - 2\Delta/m)^{1/2} \pm V]. \quad (2.11)$$

Since the thermal velocity  $V_{th}$  [equal to  $(8kT/\pi\mu)^{1/2}$  and  $T=300$  K] satisfies the condition,  $mV_{th}^2/2 \ll \Delta$ ,  $p^{\pm}$  can be approximated by

$$p^{\pm} \sim p_0 \pm mV_{th}, \quad (2.12)$$

with  $p_0 = (-2m\Delta)^{1/2}$ . Since the range  $(2mV_{th})$  of the integration over  $p$  is narrow and  $v_m(p=p_0)=0$ , we can roughly estimate the integral over  $v$  by putting  $v_m=0$  in Eq. (2.1). The analysis made above indicates that  $p_0$  can be used as a useful measure to comprehend the behavior of the cross sections against  $n$ ,  $l$ , and  $V$ .

### III. RESULTS AND NUMERICAL APPLICATIONS AND DISCUSSION

Analytic expressions for the dipole Born [ $\sigma_{J,J-1}^B(p)$ ] and dipole Glauber [ $\sigma_{J,J'}^G(p,v)$ ] DCS's are available in Refs. 5 and 6, respectively. For the convenience of later discussion, it is instructive to compare them by the ratio

$$R_{J,J'}(\xi) [= \sigma_{J,J'}^G(p,v) / \sigma_{J,J-1}^B(p)],$$

which is expressed in terms of the reduced momentum transfer  $\xi [= (2D/ea_0)p/mv]$ . Here  $D$  is the molecular dipole moment;  $e$ , the electronic charge; and  $a_0$ , the

Bohr radius. The values of  $R_{J,J'}(\xi)$  for the rotational deexcitations with  $\Delta J=1, 2$ , and 3 are shown in Figs. 1(a)–1(c). For  $\xi \leq 0.3$ , the dipole-allowed transition ( $\Delta J=1$ ) occurs most predominantly. In this region,  $\sigma_{J,J-1}^G(p,v)$  is, therefore, well approximated by  $\sigma_{J,J-1}^B(p)$ . For  $0.3 \leq \xi < 6$ ,  $R_{J,J'}(\xi)$  decreases rapidly and becomes as small as  $R_{J,J'}(\xi)$  with  $\Delta J > 1$ . In this region the use of the Born approximation is questionable, because the dipole-forbidden transitions can be expected to contribute to the same extent as the dipole-allowed transition. For  $\xi \geq 6$ , there appears an oscillatory structure in the curve  $R_{J,J'}(\xi)$  versus  $\xi$ , which might not be true and might disappear in a more sophisticated treatment including short-range potentials. However, this structure gives no serious influence on the final results of the present application.

Molecular data are listed in Table I for four polar molecules studied here. These molecules have been selected for the case studies to examine the applicability of the dipole Born DCS. The Boltzmann average of the initial  $J$  at 300 K is also given in Table II. It is discerned that the  $J$  distribution becomes broader for molecules with smaller rotational constant (see Fig. 2).

We have calculated the ionization cross sections for collisions between the Rydberg Xe atom and these polar molecules. The dependence of the cross sections on  $J$ ,  $\Delta J$ ,  $l$ ,  $n$ ,  $D$ , and collision velocity  $V$  are obtained, and are analyzed in Secs. III A–III E.

#### A. Dependence on $J$ and $\Delta J$

In order to see the  $J$  and  $\Delta J (= J - J')$  dependences of the cross sections in Eq. (2.1), we have averaged the cross sections with respect to  $l$  as follows:

$$\sigma_n(J, \Delta J; V) = \frac{1}{n^2} \sum_l (2l+1) \sigma_{nl, J, J'}(V). \quad (3.1)$$

Figure 3 shows the results for the Xe(50) + HF( $J$ ) sys-

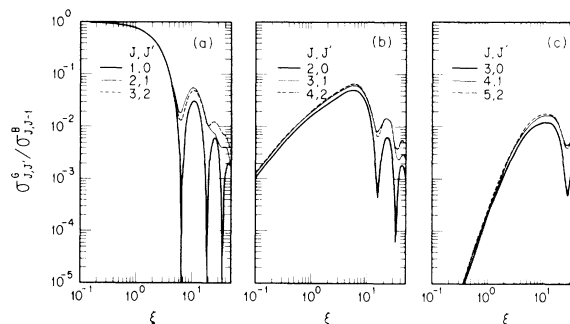


FIG. 1. Ratio of  $\sigma_{J,J'}^G(p,v)$  (Glauber approximation) to  $\sigma_{J,J-1}^B(p)$  (Born approximation) against the reduced momentum transfer  $\xi [= (2D/ea_0)p/mv]$  for (a)  $\Delta J=1$ , (b)  $\Delta J=2$ , and (c)  $\Delta J=3$ . The other cases with higher  $J$  cannot be drawn in a distinguishable way.

TABLE I. Dipole moment  $D$  and rotational constant  $B$  used in the calculation. All values are given in atomic units. Values in square brackets are the power of ten by which the entry is to be multiplied.

	CO	HCl	HF	LiF
$D$	4.41[-2]	4.36[-1]	7.19[-1]	2.49
$B$	8.76[-6]	4.76[-5]	9.37[-5]	6.08[-6]

tem with  $\Delta J=1, 2,$  and  $3$  at the thermal velocity  $V_{th}$ . Calculations have been carried out with use of  $\sigma_{J,J-1}^B(p)$  and  $\sigma_{J,J'}^G(p,v)$  for the electron-molecule scattering. As far as the magnitude of the cross section is concerned, it can be easily understood from Fig. 1 that the use of the Born DCS leads to a considerable overestimate compared to the case of the Glauber DCS and that the Glauber result decreases sharply with increasing  $\Delta J$ . In order to interpret the  $J$  dependence of the Born cross section qualitatively, we use  $p_0$  in Eq. (2.12). In the case of HF,  $p_0(\text{a.u.})=(4mBJ)^{1/2}\simeq 0.03J^{1/2}$ . This indicates that the effective integral domain of  $p$  gradually shifts to the larger  $p$  side with increasing  $J$ , and collisions with small  $p$  become less important. Thus, the decrease of the cross section with increasing  $J$  is caused by the decline (proportional to  $p^{-2}$ ) of  $\sigma_{J,J-1}^B$  as a function of  $p$ . The  $J$  dependence of the Glauber cross sections can be interpreted as follows in terms of the reduced momentum transfer  $\xi_0$  [ $= (2D/ea_0)p_0/v$ ], because the dipole Glauber DCS is expressed as a function of  $\xi$ . Setting  $v\simeq u_n(=1/50 \text{ a.u.})$ , we obtain  $\xi_0\simeq 1.5J^{1/2}$ . For  $2 < J < 10$ ,  $2.1 < \xi_0 < 4.7$ . In this range  $R_{J,J-1}(\xi)$  has a deep dip, while the other  $R_{J,J'}(\xi)$ 's have maxima. This difference appears in the  $J$  dependence of the cross sections. We can thus conclude that the decrease in  $\sigma_{50}^G(J, \Delta J=1; V_{th})$  results from the deep dip near  $\xi=7$ .

In Fig. 4, the cross sections averaged over thermal rotational distribution,

$$\sigma_n(\Delta J; V) = \sum_{J=\max(\Delta J, J^*)} f_J \sigma_n(J, \Delta J; V), \quad (3.2)$$

are plotted as a function of  $\Delta J$ . As  $\Delta J$  increases by 1, the cross section becomes smaller by one order of magnitude. This tendency is, however, not observed in the case where the  $J^*$  value satisfying the inequality of Eq. (2.7) is very large compared to  $J_{av}$ . This latter condition is realized for the cases of small  $B$  and/or low  $n$ . An example is given in Table III for the  $\text{Xe}(n)+\text{HCl}$  system. It is seen that the ionization with simultaneous dipole-forbidden rotational transitions ( $\Delta J > 0$ ) rather than dipole-allowed transitions ( $\Delta J=1$ ) occur dominantly for  $n \leq 24$ . In the present calculations, therefore, we have taken into account all the contributions from  $\Delta J=1$  to  $\Delta J=5$ .

TABLE II. The Boltzmann average  $J_{av}$  of the initial rotational quantum number  $J$  at 300 K.

	CO	HCl	HF	LiF
$J_{av}$	8.7	3.4	2.3	10.6

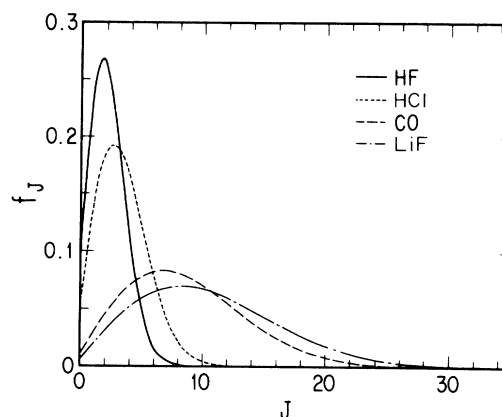


FIG. 2. Rotational distributions at 300 K for the CO, HF, HCl, and LiF molecules as a function of rotational quantum number ( $J$ ).

### B. Dependence on $l$

In Fig. 5, the cross section  $\bar{\sigma}_{nl}(V_{th})$  for the collisions of  $\text{Xe}(50l)$  with HF are plotted as a function of  $l$ . The dipole Glauber DCS is used. The increase of the cross section is seen to be gradual at small  $l$  and to be rapid at large  $l$ . As  $l$  increases, the most probable velocity  $v_{nl}$  of  $e_R(n,l)$  becomes gradually larger. Therefore, the value of  $\xi$  contributing to the cross section becomes small because  $\xi$  is inversely proportional to  $v$ . Thus the  $l$  dependence of the cross section is connected to the rapid decrease of  $R_{J,J-1}(\xi)$  in the range  $2.7 < \xi < 4.7$ . The oscillatory structure of the Rydberg electron-velocity distribution yields a small variation of the cross section as a function of  $l$ .

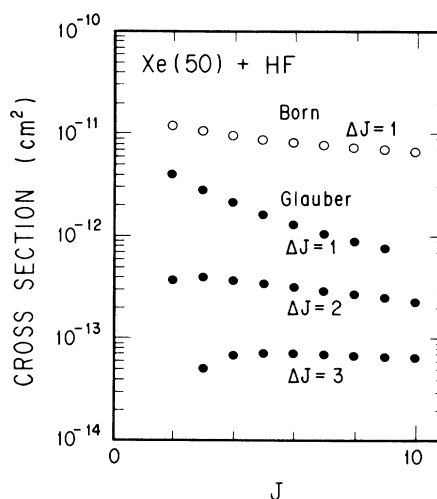


FIG. 3. Rotational quantum number ( $J$ ) dependence of cross sections for  $\text{Xe}(50) + \text{HF}(J) \rightarrow \text{Xe}^+ + e + \text{HF}(J')$  at thermal velocity ( $6.0 \times 10^4 \text{ cm/s}$ ). The cross-section values marked "Born" and "Glauber" are obtained with use of the dipole Born and dipole Glauber approximations to the  $e + \text{HF}(J) \rightarrow e + \text{HF}(J')$  scattering amplitude, respectively. Cross sections for the ionization with simultaneous dipole-forbidden transitions with  $\Delta J(=J-J') > 1$  are also shown.

TABLE III. Cross sections ( $\text{\AA}^2$ ) for ionization with simultaneous dipole-allowed and dipole-forbidden rotational deexcitation transitions for  $\text{Xe}(n) + \text{HCl} \rightarrow \text{Xe}^+ + e + \text{HCl}$  at thermal velocity ( $4.7 \times 10^4$  cm/s).  $J_{\min} = \max(\Delta J, J^*)$ . Values in square brackets are the power of ten by which the entry is to be multiplied.

$n$	Born				Glauber				Total	
	$J_{\min}$	$\Delta J=1$	$\Delta J=1$	$J_{\min}$	$\Delta J=2$	$J_{\min}$	$\Delta J=3$	$J_{\min}$		$\Delta J=4$
20	14	1.7	1.1	8	4.3[1]	6	1.0[1]	5	2.7	5.7[1]
21	12	2.3[1]	1.5[1]	7	9.4[1]	5	1.6[1]	5	2.8	1.3[2]
22	11	8.4[1]	5.4[1]	6	1.8[2]	5	1.9[1]	5	3.0	2.6[2]
23	10	2.3[2]	1.5[2]	6	1.9[2]	5	2.1[1]	4	4.0	3.7[2]
24	10	2.6[2]	1.6[2]	6	2.0[2]	5	2.2[1]	4	4.4	3.9[2]
25	9	7.1[2]	4.4[2]	5	3.6[2]	4	3.3[1]	4	4.7	8.4[2]
26	8	1.7[3]	1.1[3]	5	3.7[2]	4	3.6[1]	4	4.9	1.5[3]
27	8	1.8[3]	1.1[3]	5	3.8[2]	4	3.8[1]	4	5.1	1.5[3]
28	7	3.9[3]	2.4[3]	4	6.1[2]	4	4.1[1]	4	5.3	3.1[3]
29	7	3.9[3]	2.4[3]	4	6.2[2]	4	4.3[1]	4	5.6	3.1[3]
30	6	7.9[3]	4.9[3]	4	6.4[2]	3	5.5[1]	4	5.8	5.7[3]

### C. Dependence on $n$ and $D$ (dipole moment)

The  $n$  dependence has been investigated for the cross sections averaged over  $l$ , i.e.,

$$\bar{\sigma}_n(V) = \frac{1}{n^2} \sum_l (2l+1) \bar{\sigma}_{nl}(V). \quad (3.3)$$

Calculations have been carried out for the  $\text{Xe}(n) + \text{CO}$ ,  $\text{HCl}$ ,  $\text{HF}$ , and  $\text{LiF}$  systems with  $n \leq 100$  at  $V_{\text{th}}$ . It is noted that the dipole moment  $D$  of the molecules studied here satisfies the relation,  $D_{\text{CO}} < D_{\text{HCl}} < D_{\text{HF}} < D_{\text{LiF}}$  (see Table I).

The results  $\bar{\sigma}_n^B(V_{\text{th}})$  and  $\bar{\sigma}_n^G(V_{\text{th}})$  obtained with use of the dipole Born and dipole Glauber DCS's are shown as a function of  $n$  in Figs. 6–9. It is seen that the dipole

Glauber DCS brings about a decrease in the cross section and yields a sawlike  $n$  dependence in contrast to a clear steplike  $n$  dependence<sup>13</sup> in the case of the dipole Born DCS. This sudden increase of the cross section appears at each  $n$  at which the binding energy of the Rydberg electron ( $1/2n^2$  a.u.) becomes equal to the molecular rotational energy ( $2BJ$ ) released in the dipole-allowed deexcitation transition. In other words, as  $n$  increases, the molecules with lower  $J$  can take part in the ionization, and thus the cross section takes a rapid increase. The values of  $\bar{\sigma}_n^B(V_{\text{th}})$  and  $\bar{\sigma}_n^G(V_{\text{th}})$  become larger with increasing  $D$ , and the difference between them becomes more prominent. These features come from the sharp decrease of  $R_{J,J-1}(\xi)$  in the range  $1 < \xi < 6$ . Since the reduced momentum transfer  $\xi$  is inversely proportional to  $v$  and is proportional to  $D$ ,  $\xi_0 [= (2D/ea_0)p_0/v$  and  $v = v_n]$ , being a measure to estimate the effective domain of the twofold integral with respect to  $p$  and  $v$ , becomes larger with  $n$  and/or  $D$ . This explains the prominent difference in  $\bar{\sigma}_n^B(V_{\text{th}})$  and  $\bar{\sigma}_n^G(V_{\text{th}})$ .

### D. Dependence on $V$ (relative collision velocity)

The calculated results of  $\bar{\sigma}_{nl}(V)$  defined by Eq. (2.5) are shown in Figs. 10 and 11 for the  $\text{Xe}(27f) + \text{HF}$  and

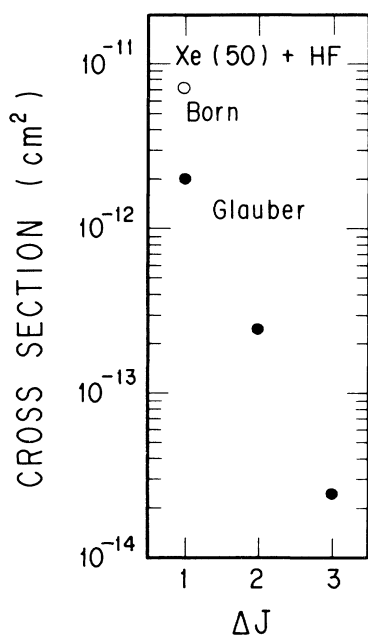


FIG. 4.  $\Delta J$  dependence of cross sections averaged over thermal rotational distribution for  $\text{Xe}(50) + \text{HF}(J) \rightarrow \text{Xe}^+ + e + \text{HF}(J')$  at thermal velocity ( $6.0 \times 10^4$  cm/s).

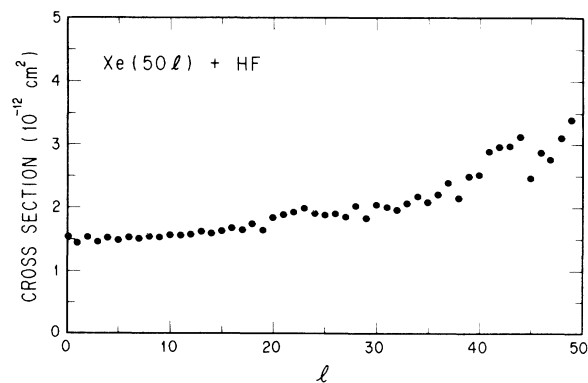


FIG. 5. Azimuthal quantum number ( $l$ ) dependence of cross sections for  $\text{Xe}(50l) + \text{HF} \rightarrow \text{Xe}^+ + e + \text{HF}$  at thermal velocity ( $6.0 \times 10^4$  cm/s).

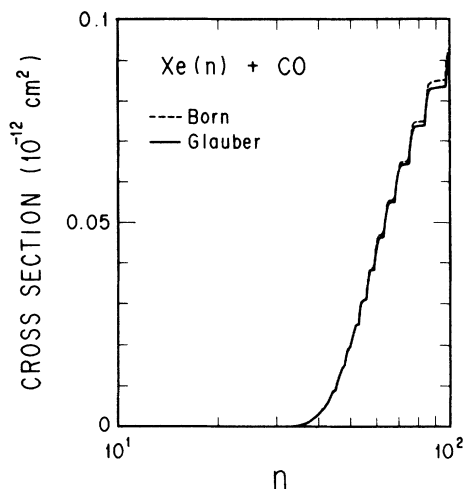


FIG. 6. Principal quantum number ( $n$ ) dependence of cross sections for  $\text{Xe}(n) + \text{CO} \rightarrow \text{Xe}^+ + e + \text{CO}$  at thermal velocity ( $5.2 \times 10^4$  cm/s).

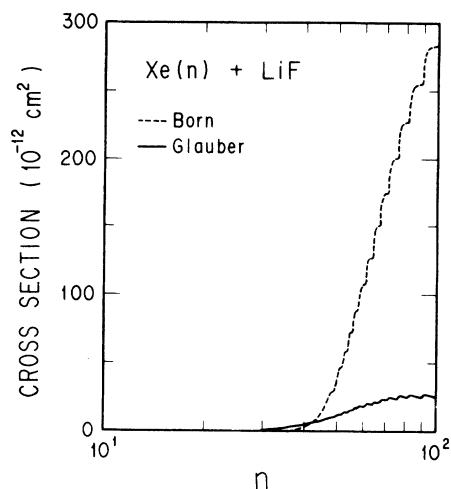


FIG. 9. The same as in Fig. 6 for  $\text{Xe}(n) + \text{LiF} \rightarrow \text{Xe}^+ + e + \text{LiF}$  at thermal velocity ( $5.4 \times 10^4$  cm/s).

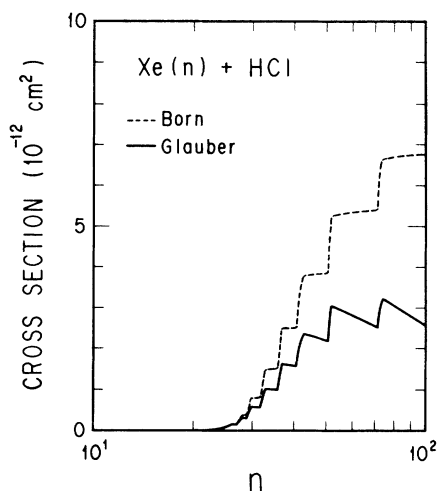


FIG. 7. The same as in Fig. 6 for  $\text{Xe}(n) + \text{HCl} \rightarrow \text{Xe}^+ + e + \text{HCl}$  at thermal velocity ( $4.7 \times 10^4$  cm/s).

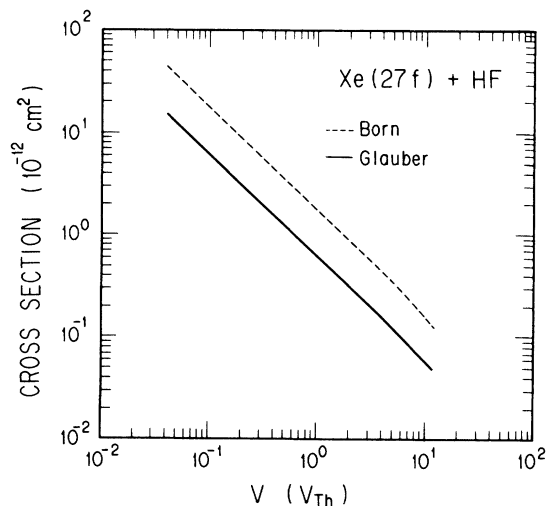


FIG. 10. Relative velocity ( $V$ ) dependence of cross sections for  $\text{Xe}(27f) + \text{HF} \rightarrow \text{Xe}^+ + e + \text{HF}$ .  $V$  is given in units of thermal velocity  $V_{\text{th}} (= 6.0 \times 10^4$  cm/s).

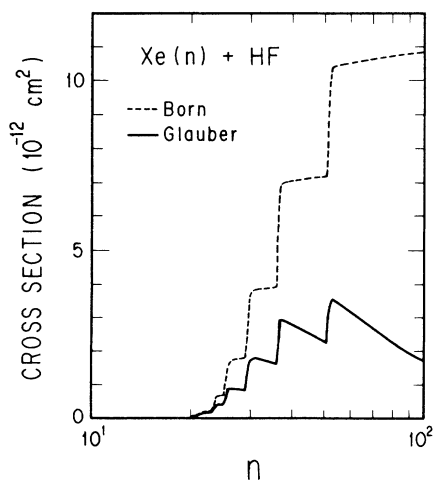


FIG. 8. The same as in Fig. 6 for  $\text{Xe}(n) + \text{HF} \rightarrow \text{Xe}^+ + e + \text{HF}$  at thermal velocity ( $6.0 \times 10^4$  cm/s).

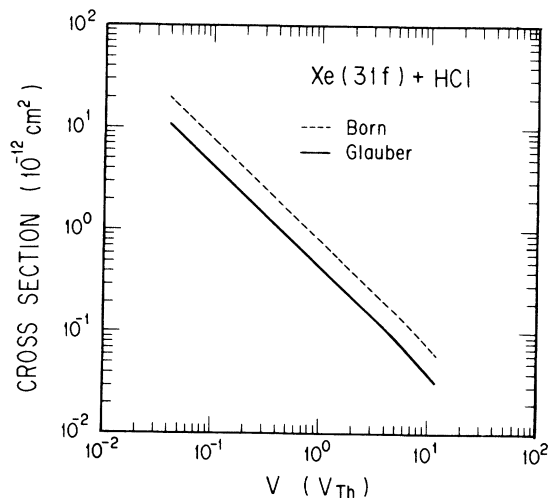


FIG. 11. The same as in Fig. 10 for  $\text{Xe}(31f) + \text{HCl} \rightarrow \text{Xe}^+ + e + \text{HCl}$  and  $V_{\text{th}} (= 4.7 \times 10^4$  cm/s).

Xe(31*f*) + HCl systems, respectively. Both results indicate that  $\bar{\sigma}_{nl}(V)$  can be expressed as  $\bar{\sigma}_{nl}(V) = C_{nl}/V$  with  $C_{nl}$  a proportionality constant. The value of  $C_{nl}$  depends on the approximation employed for the scattering amplitude of the process (1.2).

It is shown in a previous paper<sup>12</sup> that the  $V$  dependence of the cross sections is generally given as  $1/V$  in the low-velocity limit when the electron-neutral atom (molecule) DCS depends, as in the case of the Born DCS, only on the momentum transfer. In the case of the Glauber DCS, we can provide the following qualitative interpretation in terms of  $p^\pm (\sim p_0 \pm mV)$  given by Eq. (2.12). For  $V/V_{th} < 10$ , the relative velocity  $v (= |\mathbf{V} - \mathbf{u}|)$  between  $e_R$  and  $M(J)$  is nearly equal to the velocity  $u$  of  $e_R$ . This means that the energy transfer from relative translational motion to atomic excitation is much less effective. Therefore, ionization occurs mainly due to the energy transfer from molecular rotation to atomic excitation in the thermal-energy collisions. Because of this,  $p_0$  is determined only by the rotational deexcitation energy. Since the integration range  $[p^-, p^+]$  is narrow in proportion to  $V$ , we can use  $p_0$  as a representative point to estimate the integral over  $v$  in Eq. (2.1). Since  $v_m$  is zero at  $p = p_0$ , we can roughly estimate the integral over  $v$  by setting  $v_m = 0$ . Then the velocity dependence of the cross section can again be shown to be  $1/V$ . Substituting an expression  $V\bar{\sigma}_{nl}(V) = C_{nl}$  into Eq. (2.8), we can easily see that the rate constant is independent of the temperature  $T$ , i.e.,  $K_{nl}(T) = C_{nl}$ .

#### E. Comparison with experiment

In Table IV, the calculated ionization rate constants at 300 K for Xe(27*f*) + HF and Xe(31*f*) + HCl are compared with the experimental values<sup>10,11</sup> and theoretical values obtained by the classical Monte Carlo approach.<sup>4</sup> The classical results are obtained simply by  $V\bar{\sigma}_{nl}(V)$ , though the classical cross section  $\bar{\sigma}_{nl}(V)$  is not in good proportion to  $1/V$  [e.g., Fig. 7(b) in Ref. 4 shows a more moderate  $V$  dependence than  $1/V$ ]. It is seen that the Born result agrees quite well with the experimental value for Xe(27*f*) + HF, but not well for Xe(31*f*) + HCl. The contrary applies to the classical results. The results of the Glauber approximation, on the other hand, are smaller in both cases, although the ratio between the two cases agrees very well with that of the experiment (see the last row of Table IV).

#### IV. SUMMARY AND CONCLUSION

Ionization collision between Rydberg atoms and polar molecules was investigated within the semiquantal approximation. A comparative study was made by employing the dipole Born and dipole Glauber approximations for the electron-polar molecule scattering. Analysis was made for the dependences of the cross sections on the following various quantities: relative collision velocity, initial rotational state  $J$ , rotational quantum number change, principal quantum number, azimuthal quantum number, and dipole moment.

For the Xe( $n$ ) + CO system, there is almost no discrepancy between the two results of the Born and Glauber approximations. As the molecular dipole moment becomes larger and/or the principal quantum number increases, however, there appears a larger discrepancy between the two results and the Born approximation seems to lead to a considerable overestimate. This discrepancy stems from the fact that the dipole Glauber DCS for the dipole-allowed transitions decreases rapidly as a function of reduced momentum transfer compared to the dipole Born DCS. A clear steplike  $n$  dependence obtained in the Born approximation is replaced by a sawlike  $n$  dependence when the Glauber approximation is employed. The interaction range between Rydberg electron and polar molecule is short compared to that between free electron and polar molecule because of the charge neutrality. Therefore, the forward scattering with small momentum transfer does not contribute appreciably to the collision process (1.1) between a Rydberg atom and a molecule. This situation makes the use of the Born DCS questionable except in the case of extremely weak polar molecules. Thus it is probably allright to say that the Glauber results are more reliable than the Born results.

In order for the lowly excited Rydberg atoms to be ionized in collisions with molecules by a simultaneous dipole-allowed transition ( $\Delta J = 1$ ), the molecules should be in high- $J$  states because the energy transfer  $2BJ$  ought to be larger than the ionization potential  $\epsilon_n$ . The population of such a molecule is, however, exponentially small. Thus the ionization with simultaneous dipole-forbidden transitions ( $\Delta J > 1$ ) becomes rather dominant in thermal collisions involving lowly excited Rydberg atoms because the necessary energy transfer  $\epsilon_n$  [ $= \Delta J(2J + 1 - \Delta J)B$ ] can be attained by relatively small  $J$ 's. This tendency was actually observed in the recent

TABLE IV. Experimental and theoretical ionization rates (in  $10^{-7}$  cm<sup>3</sup>/s) at 300 K for the Xe(27*f*) + HF and Xe(31*f*) + HCl systems. The values in parentheses are the experimental and theoretical (statistical) uncertainties. The values marked (Born) and (Glauber) are obtained with use of the dipole Born and dipole Glauber approximations to  $e + \text{HF}$  (or HCl) scattering amplitude, respectively.

	Experiment		Theory	
Xe(27 <i>f</i> ) + HF	1.5(±0.8) <sup>a</sup>	1.36 (Born)	0.480 (Glauber)	0.22(±0.02) <sup>b</sup>
Xe(31 <i>f</i> ) + HCl	0.9(±0.4) <sup>c</sup>	0.480 (Born)	0.265 (Glauber)	0.76(±0.08) <sup>b</sup>
Ratio	1.7	2.8	1.8	0.29

<sup>a</sup>Reference 10.

<sup>b</sup>Reference 4.

<sup>c</sup>Reference 11.

experiment by Pesnelle *et al.*<sup>7</sup> Theoretical studies on this problem will be published in a forthcoming paper.

It was shown that the cross section is almost inversely proportional to the relative velocity in the semiquantal approximation and thus the ionization rate constant is almost independent of temperature. Experimental investigation on this dependence would be very intriguing. In spite of our expectation that the Glauber approximation should be more accurate than the Born approximation, the experimentally observed ionization rates for the Xe(27*f*) + HF and Xe(31*f*) + HCl systems agree better with the Born results than with the Glauber results, al-

though the ratio between the two systems agrees well with that of the Glauber approximation. The reason for this discrepancy is not clear.

#### ACKNOWLEDGMENTS

We gratefully thank Professor M. Matsuzawa of The University of Electro-Communications for useful discussions. One of us (T.S.) would like to express his thanks to Dr. N. Shikazono, Dr. S. Igarasi, and Dr. Y. Nakai of Japan Atomic Energy Research Institute for their encouragement during this work. Part of this work was done while T. S. was at Argonne National Laboratory.

---

<sup>1</sup>A recent comprehensive review is found in *Rydberg States of Atoms and Molecules*, edited by R. F. Stebbings and F. B. Dunning (Cambridge University, Cambridge, 1983).

<sup>2</sup>F. G. Kellert, K. A. Smith, R. D. Rundle, F. B. Dunning, and R. F. Stebbings, *J. Chem. Phys.* **72**, 3179 (1980); F. B. Dunning and R. F. Stebbings, in Ref. 1, p. 315, and references therein.

<sup>3</sup>M. Matsuzawa, in Ref. 1, p. 267, and references therein.

<sup>4</sup>S. Preston and N. F. Lane, *Phys. Rev. A* **33**, 148 (1986).

<sup>5</sup>K. Takayanagi, *J. Phys. Soc. Jpn.* **21**, 507 (1966); O. H. Crawford, *J. Chem. Phys.* **47**, 1100 (1967).

<sup>6</sup>O. Ashihara, I. Shimamura, and K. Takayanagi, *J. Phys. Soc. Jpn.* **38**, 1732 (1975); I. Shimamura, in *Electron-Molecule Collisions*, edited by I. Shimamura and K. Takayanagi (Plenum, New York, 1984), p. 89.

num, New York, 1984), p. 89.

<sup>7</sup>A. Pesnelle, C. Ronge, M. Perdrix, and G. Watel, *Phys. Rev. A* **34**, 5146 (1986).

<sup>8</sup>M. R. Flannery, in Ref. 1, p. 393, and references therein.

<sup>9</sup>T. Shirai, Y. Nakai, and H. Nakamura, *Phys. Rev. A* **30**, 1672 (1984), to be referred to as I.

<sup>10</sup>C. Higgs, K. A. Smith, G. B. McMillian, F. B. Dunning, and R. F. Stebbings, *J. Phys. B* **14**, L285 (1981).

<sup>11</sup>R. F. Stebbings, F. B. Dunning, and C. Higgs, *J. Electron Spectrosc. Relat. Phenom.* **23**, 333 (1981).

<sup>12</sup>H. Nakamura, T. Shirai, and Y. Nakai, *Phys. Rev. A* **17**, 1892 (1978).

<sup>13</sup>M. Matsuzawa and W. A. Chupka, *Chem. Phys. Lett.* **50**, 373 (1977).